Polymer Journal (2015) 47, 753–759

www.nature.com/pj

ORIGINAL ARTICLE

A new conjugated poly(pyridinium salt) derived from phenanthridine diamine: its synthesis, optical properties and interaction with calf thymus DNA

Yujiao Sun[1], Jing Wang[2], Lu Jin[1], Ying Chang[1], Jingjing Duan[1] and Yan Lu[1]

A new conjugated poly(pyridinium salt) derivative (P1) containing heterocyclic phenanthridine moieties in the main chain with tosylate counterions was prepared via a ring-transmutation polymerization reaction. Its chemical structure was established using NMR and FTIR spectra. Its number-average molecular weight (M_n) and polydispersity were 14 430 and 1.456, respectively, as determined by gel permeation chromatography (GPC). The interaction of P1 with calf thymus DNA (ctDNA) in an ethanol-Tris-HCl buffer (2 mM, pH 7.4) (v/v = 1:1) was investigated by ultraviolet–visible, fluorescence, circular dichroism spectroscopy, and dynamic light scattering (DLS) measurements. The electrostatic attraction and intercalation interaction between P1 and ctDNA resulted in a significant fluorescence quenching of polymer P1 in the ethanol–Tris-HCl buffer, and the ratio of fluorescence intensity at 523 nm in the absence of ctDNA (F_0) to that in the presence of ctDNA (F_i) was linearly proportional to the concentration of ctDNA within the range of 0–6.0 μM. Therefore, the conjugated polyelectrolyte is expected to be used as a new fluorescent probe for the label-free detection of DNA.
Polymer Journal (2015) **47,** 753–759; doi:10.1038/pj.2015.62; published online 2 September 2015

INTRODUCTION

Conjugated polyelectrolytes (CPEs) have become a subject of extensive research for chemosensors and biosensors.[1–5] Because the π–π electrons in the conjugated backbones are delocalized, CPEs present molecular wire effects that can provide targeted signal amplification.[6,7] However, CPE optoelectronic properties can be greatly perturbed by the local electrochemical environment.[8–16] Cationic-conjugated polyelectrolytes have been widely used as DNA biosensors by taking advantage of the electrostatic interaction with the oppositely charged phosphate groups of the target polynucleotide.[17–23] Among these polyelectrolytes, cationic poly(*para*-phenylene vinylene),[24] polythiophene derivatives[25–27] and poly(fluorene-*co*-phenylene) derivatives[28–36] are widely used. The poly(fluorene-*co*-phenylene) derivatives have become particularly popular because they show a relatively high-emission quantum yield in aqueous solutions and emit blue light, and their structures can be easily modified through substitution at the C9 fluorene position.[37] Various protocols have been developed, largely by Bazan *et al.*, to detect DNA using cationic poly(fluorene-*co*-phenylene)s as biosensors. Many of these protocols are based on Förster resonant energy transfer, which requires a costly, complex and long-running operation.[20,28–36] Thus, the development of new CPE systems for sensitive DNA detection is still required.

Recently, we developed a poly(pyridinium salt)s-based bio-sensing system for the sensitive detection of biological molecules, including DNA and heparin, by taking advantage of their good photoelectric characteristics and their charged nature.[38–41] Unlike common *p*-conjugated polyelectrolytes, which are characterized by a backbone with a delocalized electronic structure and the charged functional side chains, poly(pyridinium salt)s belong to a class of main-chain cationic polymers and consist of 4,4′-(1,4-phenylene)bis(2,6-diphenylpyridinium) ions along the backbone of the polymer chains. They exhibit a number of interesting photoelectrical properties such as redox behavior, liquid crystalline (LC) properties and light-emitting properties, which have been investigated quite extensively by Bhowmik *et al.*[42–45] In the present study, we designed and synthesized a new poly(pyridinium salt)s derivative that contains heterocyclic phenanthridine moieties in the main chain with tosylate counterions (**P1**), and we studied its interaction with calf thymus DNA by ultraviolet (UV)–visible (Vis) and fluorescence spectra, dynamic light scattering (DLS) and circular dichroism (CD) spectra.

MATERIALS AND METHODS

Materials and measurements

All chemical reagents were commercially available and used as received unless otherwise stated. Calf thymus DNA was purchased from Beijing Sunbiotech Co. Ltd (Beijing, China). The DNA concentration was determined by absorption spectroscopy by using the molar absorption coefficient ($\varepsilon = 6600\ M^{-1}\,cm^{-1}$) at 260 nm. Milli-Q water (18.2 MΩ) was used for all the experiments.

^{1}H NMR spectra were collected on a Bruker Avance III-400 NMR spectrometer (Bruker Co., Billerica, MA, USA) (400 MHz). d_6-dimethyl sulfoxide

[1]Department of Functional Materials, School of Materials Science and Engineering, Tianjin University of Technology, Tianjin, China and [2]Tianjin Key Laboratory for Photoelectric Materials and Devices, School of Materials Science and Engineering, Tianjin University of Technology, Tianjin, China
Correspondence: J Wang or Professor Y Lu, School of Materials Science and Engineering, Tianjin University of Technology, No. 391 Binshui West Road, 300384 Tianjin, China.
E-mail: wangjing@iccas.ac.cn or luyan@tjut.edu.cn
Received 29 April 2015; revised 10 June 2015; accepted 29 June 2015; published online 2 September 2015

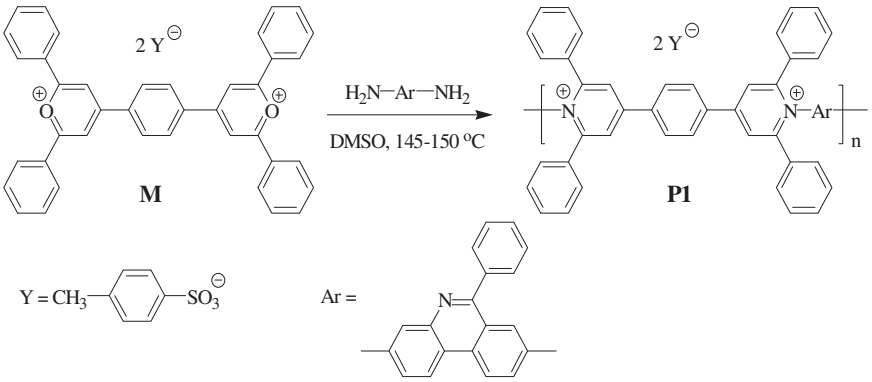

Scheme 1 Synthesis of poly(pyridinium salt)s derivative (**P1**).

(DMSO) was used as solvents and tetramethylsilane as internal standard. GPC analysis was conducted with a Waters 2690 liquid chromatography system equipped with a Waters 996 photodiode detector and Phenogel GPC columns. Linear polystyrene standards were applied for calibration. The eluent was DMF with 0.01 M LiBr at a flow rate of 1 ml min^{-1} at 35 °C. A total of 50 µl of 0.2 wt % of polymer in DMF containing 0.01 M LiBr was injected into the columns. The pH was measured on a Mettler-Toledo Delta 320 pH meter (Mettler-Toledo International Inc., Greifensee, Switzerland). DLS measurements were performed using a Zetasizer Nano ZS90 (Malvern Instruments Co., UK) equipped with a He–Ne laser. All CD spectra were measured on a Jasco J-715 WI spectropolarimeter (Jasco Co., Tokyo, Japan) using a cylindrical quartz cell with a pathlength of 10 mm. The absorption spectrum was recorded on a Shimadzu UV-2550 spectrometer (Shimadzu Co., Tokyo, Japan). Fluorescence was measured on a Hitachi F-4600 fluorescence spectrophotometer (Hitachi Co., Tokyo, Japan) equipped with a xenon lamp excitation source.

Synthesis of bis(pyrylium salt)s monomer (M)

The 4,4'-(1,4-phenylene)bis(2,6-diphenylpyrylium)ditosylate, **M**, was synthesized according to the procedure reported elsewhere, (see Supplementary Scheme S1)[42–45] and a detailed synthetic procedure is also provided for its preparation in the ESI.

Polymer synthesis

The bis(pyrylium) salt, **M**, was reacted with 6-phenyl-phenanthridine-3,8-diamine by a ring-transmutation polymerization reaction to yield the desired polymer **P1** according to the previously reported procedure.[42] An equal molar ratio of the monomer **M** and diamine was placed in DMSO in a three-necked, round-bottomed flask equipped with a magnetic stirrer. Approximately 5 ml toluene was added to distill the water that was generated in the reaction as a toluene–water azeotrope, and this process was facilitated by using a Dean–Stark trap and water condenser. The temperature was monitored with a thermometer and adjusted to 145–150 °C. The reaction was kept under nitrogen atmosphere for 48 h. Upon completion, the reaction mixture was allowed to cool to room temperature. The DMSO was subsequently removed from the reaction mixture under vacuum to form a viscous polymer solution. The polymer solution was then poured into ethyl acetate to precipitate the polymer, which was collected via filtration. The resulting polymer was dried under vacuum at 110 °C for 72 h. ^{1}H NMR (400 MHz, d_6-DMSO, p.p.m.): 8.85 (*d*, 4H, aromatic meta N^+), 8.66 (*s*, 4H, 1,4-phenylene), 8.39 (*s*,1H), 8.26—7.05 (*m*, 38H, phenyl), 2.26 (6H, *s*, -C*H*$_3$).

RESULTS AND DISCUSSION

Synthesis and characterization of P1

Scheme 1 outlines the reaction sequence that was utilized to synthesize the poly(pyridinium salt)s derivative **P1**. The comonomer **M** was easily synthesized according to the literature in high yield (87 %) by treating tetraketone with triphenylmethanol and *p*-toluenesulfonic acid.[42–45] The conjugated poly(pyridinium tosylate)s (**P1**) was prepared by the ring-transmutation polymerization reaction, which was performed by heating the reactants in DMSO, as previously reported.[38–45] In this polymerization reaction, it is important to remove the water generated by the transformation of the pyrylium rings to the pyridinium rings from the polymerization medium. Thus, toluene was added into the reaction system to remove the water generated during the polymerization process as a toluene/water azeotrope, and excess toluene were removed by distillation. The reaction mixtures were heated at 145–150 °C for additional 48 h. The polymer **P1** was essentially isolated in quantitative yield by precipitation with the addition of ethyl acetate.

^{1}H NMR was employed to characterize the structure of polymer **P1**. The ^{1}H NMR spectrum of polymer **P1** in DMSO-d_6 contained aromatic absorption between 7.0 and 9.0 p.p.m., pyridinium ring absorptions between 8.0 and 9.0 p.p.m., and CH_3 absorption at 2.26 p.p.m. (Supplementary Figure S1, ESI). As shown in Supplementary Figure S1, the integration ratio of peak area for the proton signals from H_a in pyridium salts relative to that of the proton signals from H_b in phenathridine ring is approximately 4:1, which is consistent with its proposed structure. The FT–IR spectrum shows that the main absorption bands of **P1** are at 1616.8 and 1546.4 cm^{-1}, which correspond to the stretching vibration of C=C within the aromatic rings; 1360.3, 1186.4, 1116.8 and 1006.9 cm^{-1}, which correspond to the stretching vibration of C=N; and 815.3, 756.9 and 676.1 cm^{-1}, which correspond to the out-of-plane bending vibration of C-H within the aromatic rings (Supplementary Figure S2, ESI). The results of ^{1}H NMR and FT–IR are in agreement with the proposed structure. The weight- and number-average molecular weights of polymer **P1**, as determined by gel permeation chromatography (GPC) in DMF (LiBr), are 21010 and 14430, respectively, with a polydispersity index (PDI) of 1.456 (Supplementary Figure S3, ESI).

Solubility of the polymer

Being water soluble is essential for a polymer to interface with biological substrates such as proteins and DNA. Thus, the solubility of the synthesized poly(pyridinium salt)s derivative **P1** was carefully investigated. **P1** is soluble in common solvents, such as DMSO (~53 mg l^{-1}), DMF (~61 mg l^{-1}), C_2H_5OH (~2.0 mg l^{-1}), and pure H_2O (~1.3 mg l^{-1}), despite the rigid-rod structure, and this solubility should be attributed to the all *para*-catenated backbones. In contrast to the $^-BF_4$ counterion, the presence of a bulky tosylate counterion in the polymer increased its solubility in polar solvents by significantly reducing the strong ionic interactions between positive and negative charges. [42] This organic counterion provides a mechanism to increase its solubility to such an extent that it exceeds the concentration

required by spectrum detection to form a homogeneous aqueous solution in the presence of trace amount of DMSO (approximately one thousandth of the total volume).

Optical properties

The photophysical properties of **P1** in different solvents were investigated. As shown in Figure 1, **P1** exhibited similar absorption spectra in THF, DMSO, and water, with absorption peaks at 333, 344 and 342 nm, respectively, that were assigned to the π–π^* transition of the conjugated polymer backbone. In contrast, **P1** displayed different emission spectra in different solvents, with main emission peaks at 404 nm in THF, 438 nm in DMSO, and 516 nm in water. The obvious bathochromic shift of emission spectra could be attributed to the enhanced intramolecular charge transfer of **P1** in the excited state and aggregation of the polymer main chain with increased solvent polarity from THF to water. [46–48]

Because the aqueous medium is essential for studying the interaction of conjugated polyelectrolytes with biological substrates such as proteins and DNA, we examined the fluorescence of **P1** in water with varying amounts of DMSO to further understand its aqueous fluorescent properties. As shown in Figure 2, the emission peak blue shifted gradually by 78 nm, from 517 to 439 nm, when the DMSO content increased from 0 to 100% (v/v). In contrast, the emission intensity changed in a complicated manner. When the DMSO content increased from 0 to 20% (v/v), the emission intensity increased gradually. When further increasing the DMSO content to 50%, the emission intensity decreased gradually. With subsequently increases in the DMSO content, the emission intensity increased gradually again and reached the maximum at ~100% DMSO (v/v). We propose that the emission peak is dominated by the effect of intramolecular charge transfer and the configuration of polymer **P1,** whereas the emission intensity is mainly attributed to the synergistic effect of polymer aggregation and the viscosity of the mixture solvent.[48–50] Owing to interchain hydrophobic interactions, **P1** tends to aggregate in water, which quenches the concentrate and consequently lowers emission intensities. Adding DMSO to the **P1** aqueous solution increased the viscosity of the medium, resulting in higher emission intensities by inhibiting the nonradiative decay of the polymer in the excited state because the rotation and distortion of polymer were hindered in media with higher viscosities.

To explore the practical applicability of **P1**, the effect of pH on the fluorescence spectra of **P1** was also investigated. As shown in Figure 3, the fluorescence intensities of **P1** decreased gradually with increasing pH values. Under acidic conditions (pH < 6), all N atoms within **P1** may be protonated, and the intermolecular repulsion will lead to the de-aggregation of polymer chains, which should be responsible for the higher emission intensity. When pH > 10, the quaternary ammonium cations (Nc+) of **P1** may form an NcOH complex, which can enhance the π–π stacking interaction between polymer chains, resulting in lower emission intensity. The obvious blueshift of emission peaks could be attributed to the weakened intramolecular charge transfer effect of **P1** in the excited state due to the formation of an NcOH complex at pH > 10. **P1** showed stable fluorescence emission, with negligible change of emission intensity and wavelength in the pH range of 6.0–10.0. Therefore, **P1** can be used effectively at pH values near physiological conditions, which is required to detect bio-relevant targets.

UV-Vis spectroscopy analysis of P1 complexes with ctDNA

The interaction between **P1** and ctDNA was first examined by probing the UV-Vis spectra changes of **P1** when titrated with ctDNA. Because **P1** is a cationic conjugated polyelectrolyte, whereas ctDNA carries highly electronegative charges on its phosphate groups; thus, they can form complexes through electrostatic interactions. As shown in Figure 4, polymer **P1** exhibits a maximal absorption at 343 nm ($\varepsilon = 6.13 \times 10^4$ M^{-1} cm^{-1}). Upon gradually addition of ctDNA, the absorbance of polymer **P1** at 343 nm decreased gradually, whereas the change of absorption peak was negligible, indicating that an aggregation between the **P1** and ctDNA formed and that the attractive electrostatic interaction of **P1** with ctDNA does not obviously change the conformation of **P1**. Job's plot based on the UV-Vis absorption data shows a nearly 1:1 stoichiometry for the ctDNA-**P1** complex (Supplementary Figure S4).

DLS analysis of the P1 complexes with ctDNA

To demonstrate the aggregation behavior between **P1** and ctDNA, DLS experiments were performed in an ethanol–Tris-HCl buffer. The DLS data obtained for a fixed concentration of **P1** (10 μM) with varying concentrations of ctDNA (0–8 μM) show changes in the hydrodynamic diameter depending on the level of titration (Figure 5). **P1** formed small aggregates with a mean diameter of 295 nm, which is ascribed to its poor water solubility in aqueous solutions. With increasing concentrations of ctDNA, the hydro-

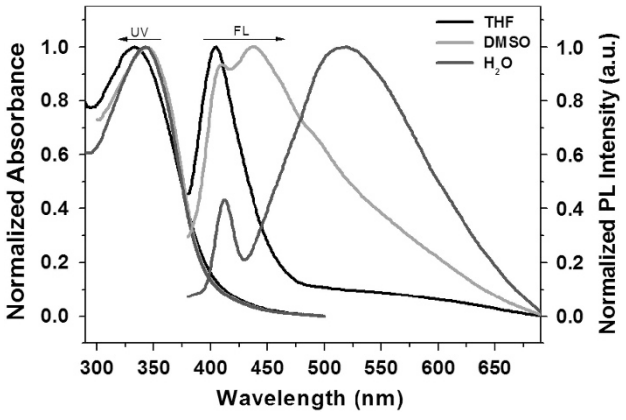

Figure 1 Absorption and fluorescence spectra of polymer **P1** in various solvents (10 μM, excitation at 360 nm). A full color version of this figure is available at *Polymer Journal* online.

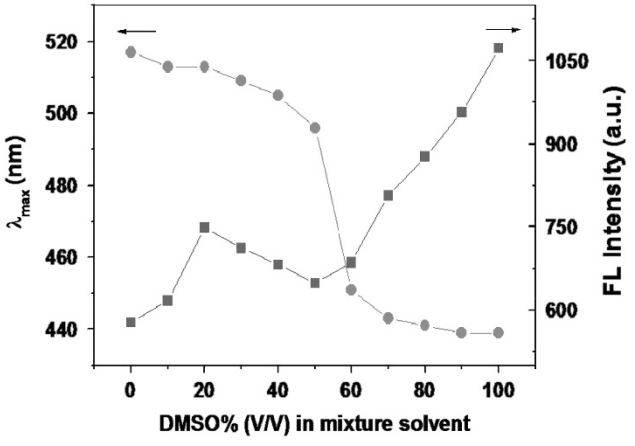

Figure 2 Fluorescence intensity and emission peak of **P1** as a function of water content in DMSO. $\lambda_{ex} = 360$ nm, [**P1**] = 10 μM. A full color version of this figure is available at *Polymer Journal* online.

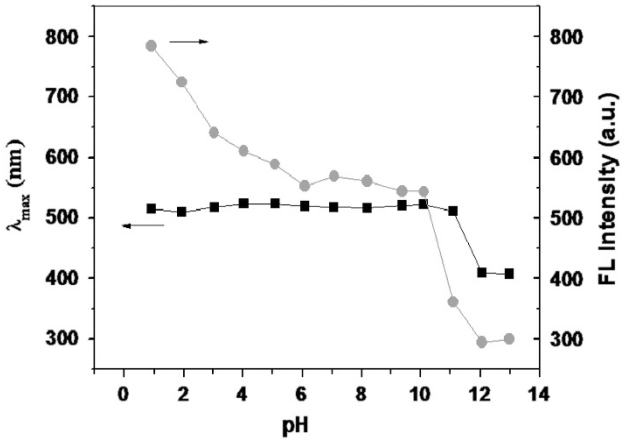

Figure 3 Effect of pH on the fluorescence intensity and emission wavelength of **P1** (10 μM) in aqueous solution. Excitation at 360 nm, [**P1**] = 10 μM. A full color version of this figure is available at *Polymer Journal* online.

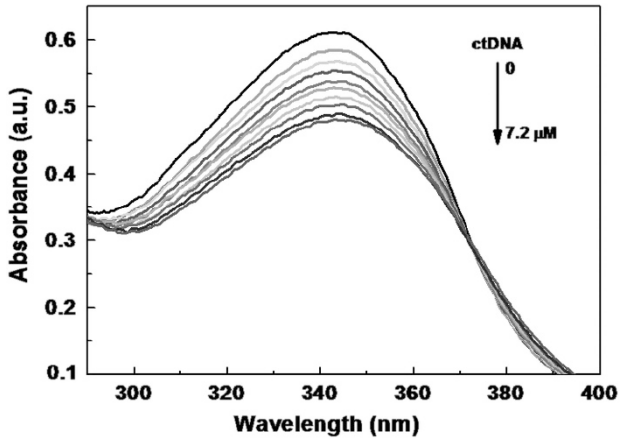

Figure 4 Absorption spectra of **P1** in the presence of various concentration of ctDNA in an ethanol–Tris-HCl buffer (2 mM, pH 7.4) (v/v = 1:1). [ctDNA] = 0, 0.8, 1.6, 2.4, 3.2, 4.0, 4.8, 5.6, 6.4, and 7.2 μM, [**P1**] = 10 μM. A full color version of this figure is available at *Polymer Journal* online.

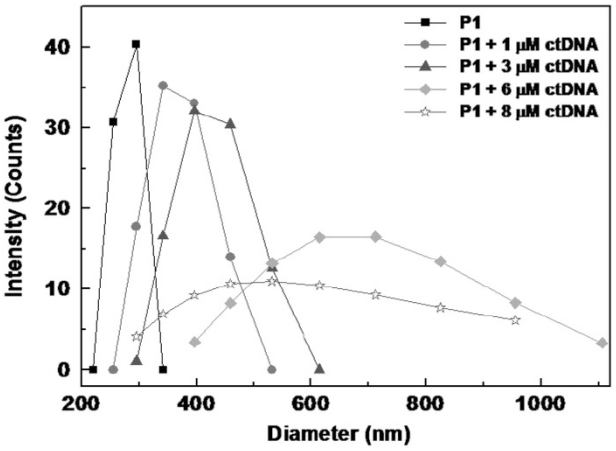

Figure 5 Hydrodynamic diameter of **P1** (10 μM) in the presence of ctDNA in an ethanol-Tris-HCl buffer (2 mM, pH 7.4) (v/v = 1:1) obtained from DLS. A full color version of this figure is available at *Polymer Journal* online.

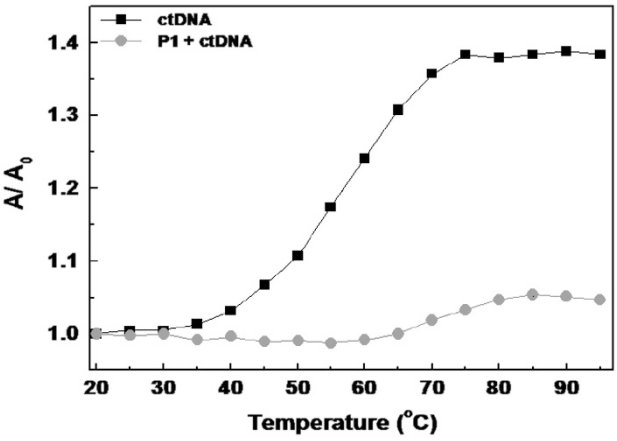

Figure 6 ctDNA (30 μM) melting curves at 260 nm in the absence and presence of **P1** (10 μM) in aqueous solution. A_0 and A denote the initial absorbance and the recorded absorbance at different temperatures, respectively. A full color version of this figure is available at *Polymer Journal* online.

dynamic diameter of the aggregates increased gradually and reached a maximum mean diameter of 712 nm at [ctDNA] = 6 μM. Thus, near the endpoint of the titration, **P1**-ctDNA complexes exist in a highly aggregated state, whereas further addition of ctDNA causes electrostatic repulsion between ctDNA; thus, the ctDNA-**P1** complexes disperse.

Thermal denaturation studies

To further analyze **P1** binding to ctDNA, the UV-melting transitions were measured with a Shimadzu UV-2550 spectrometer fitted with a water-bath apparatus to control the temperature. The melts were monitored at 260 nm, and scans were made from 20 to 95 °C. Values for the melting temperature (T_m) were defined as the temperature at which the absorbance of DNA at 260 nm reached 50% of the maximal value. Figure 6 shows the ctDNA melting curves in the presence and absence of polymer **P1**. The ctDNA 'melts,' that is, undergoes a double-to-single strand transition at 57.0 °C. The melting curve undergoes a higher temperature shift in the presence of **P1** at a concentration as low as 10 μM, resulting in an increase in the melting point by 13.8 to 70.8 °C. This finding demonstrates that polymer **P1** binding to ctDNA stabilizes the duplex structure of the latter.

Circular dichroism measurements on the complex

The objective of the CD investigation was to identify structural alterations in the ctDNA when it is bound to the conjugated polyelectrolyte **P1**. The bands due to base stacking (275 nm) and right-handed helicity (248 nm) are very sensitive to the solution structure of DNA and the conformation twist of the double helix produced by the formation of supramolecular aggregates.[51–53] Thus, CD spectroscopic analyses were performed in ethanol–Tris-HCl buffers of ctDNA in the absence and presence of **P1**. Concentrations were chosen below the point of precipitation (for example, 10 μM of ctDNA was examined in the presence of up to 10 μM **P1**). The intrinsic CD activity of the **P1** was recorded and found to be negligible. As shown in Figure 7, the CD spectrum of ctDNA in the absence of **P1** was of typical B-form, which exhibited a positive cotton effect at 275 nm and a negative cotton effect at 248 nm. Upon the addition of polymer **P1**, the intensity of the negative peak in the CD spectrum at

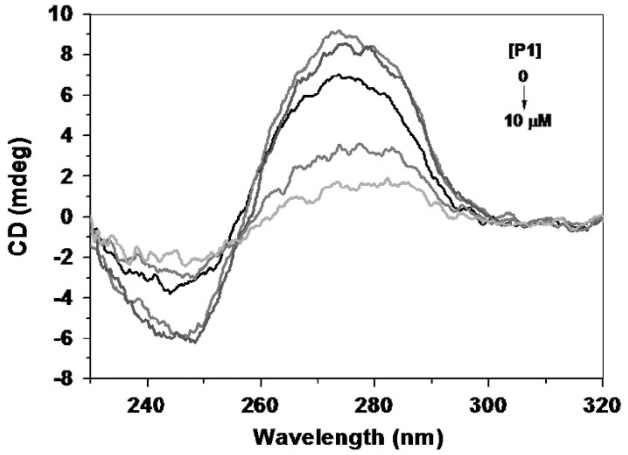

Figure 7 Circular dichroism spectra of ctDNA (10 μM) in an ethanol–Tris-HCl buffer (2 mM, pH 7.4) (v/v = 1:1) upon the addition of polymer **P1**. [**P1**] = 0, 4, 6, 8, and 10 μM. A full color version of this figure is available at *Polymer Journal* online.

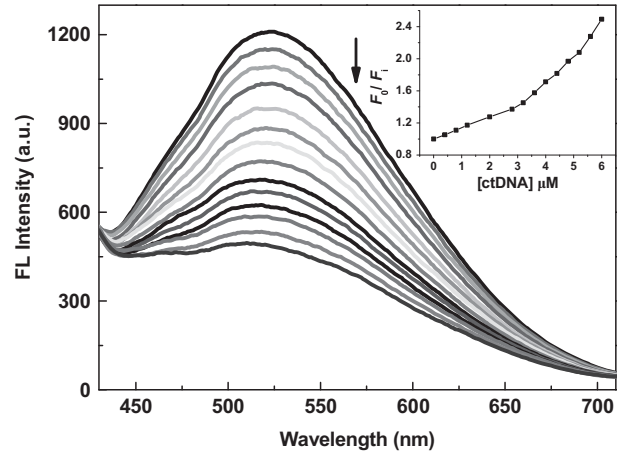

Figure 8 Fluorescence titration spectra of **P1** (10 μM) in an ethanol–Tris-HCl buffer (2 mM, pH 7.4) (v/v = 1:1) in the presence of various concentration of ctDNA. [ctDNA] = 0, 0.4, 0.8, 1.2, 2.0, 2.8, 3.2, 3.6, 4.0, 4.4, 4.8, 5.2, 5.6, and 6.0 μM. λ_{ex} = 360 nm. A full color version of this figure is available at *Polymer Journal* online.

248 nm and the positive peak at 275 nm decreased as the concentration of **P1** increased from 0 to 10 μM, indicating a significant change in conformation of the ctDNA structure as **P1** bound to the duplex.

Changes in the intensity of the CD peak at 248 nm are associated with an alteration of the hydration of the helix in the vicinity of phosphate or the ribose ring as the ionic concentration is altered.[54] Thus, exchanging a cationic polymer, such as **P1**, with a sodium ion might lead to changes in hydration near the phosphate group of the DNA helix. The decrease in the 248 nm band observed may reflect such hydration changes.[54] However, changes in the intensity of the CD peak at 275 nm should be attributed to the intercalation interaction between the phenyl groups on the side chain of polymer **P1** and the DNA base pair via hydrophobic forces. Therefore, the strong electrostatic attraction and intercalation interaction should be responsible for the binding of ctDNA with **P1**.

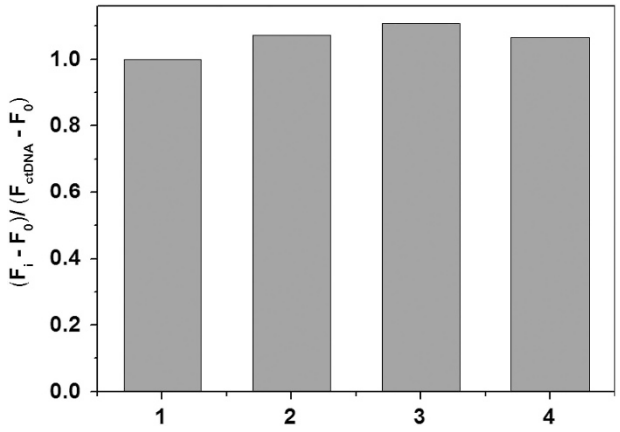

Figure 9 The $((F_i–F_0)/(F_{ctDNA}–F_0))$ ratio of fluorescence intensity at 523 nm of **P1** (10 μM) in an ethanol (EtOH)–Tris-HCl buffer (2 mM, pH 7.4) (v/v = 1:1) upon the addition of 6 μM of ctDNA in the presence of an equal concentration of competing anions. F_0 is the fluorescence intensity of free **P1**, F_i is the recorded fluorescence intensity of complexes of **P1** with various DNA molecules, F_{ctDNA} is the fluorescence intensity of the **P1**-ctDNA complex. λ_{ex} = 360 nm. Interfering species: (1) none, (2) DNA-1, (3) DNA-2, and (4) DNA-3 (DNA-1: (5′-GGTGGCCATTACCTTTGACTCTTC-3′; DNA-2: 5′-CCACCTGTTGGTAGTCCTTGTATTTAGTATCATC-3′; DNA-3: 5′-TGGTTCACG TAGTGGGCCATC-3). A full color version of this figure is available at *Polymer Journal* online.

Fluorescence study of P1 complexes with ctDNA

Addition of ctDNA to **P1** (10 μM) in ethanol–Tris-HCl buffer solution results in the fluorescence quenching of polymer **P1** (Figure 8). As the ctDNA concentration increased from 0 to 6.0 μM, the photoluminescence (PL) intensity of the cationic conjugated polyelectrolyte decreased to only one-third of the PL intensity in the absence of ctDNA, which is concomitant with the slight blueshift of the **P1** emission maximum from 523 to 511 nm. The intensity peak of the fluorescence spectrum at 523 nm was selected to investigate the analytical performance of our proposed fluorescence quenching system. Fluorescence quenching efficiencies can be quantified by the use of the Stern–Volmer equation:[55]

$$F_0/F_i = 1 + K_{SV}[Q] \quad (1)$$

where F_0 and F_i are the fluorescence intensities in the absence and presence of quencher, respectively, and [Q] is the quencher concentration. The Stern–Volmer constant, K_{SV}, provides a direct measure of the quenching efficiency and is determined from the linear portion of a plot of F_0/F_i versus [Q].

The Stern–Volmer plot of **P1** quenched by ctDNA is shown in Figure 8 as an inset. At ctDNA concentrations ranging from 0 to 6.0 μM, a linear plot with $K_{SV} = 2.21 \times 10^5$ M^{-1} ($R = 0.981$) was obtained. This quenching efficiency is pronounced if one considers a fluorescence quenching system of small molecular weight stilbene and methylviologen, whose K_{SV} is as low as 15. The extremely large quenching efficiency is caused by two separated effects as follows. First, the negatively charged ctDNA molecules are expected to readily bind positively charged conjugated polymer chains through a combination of coulombic and entropic interactions, which brings about an effect of local concentration enhancement of **P1**. This local enhancement improves the accessibility and thus the sensitivity of **P1** to ctDNA. Second, the conjugated polyelectrolyte is characterized by a 'molecular wire' effect. An isolated conjugated polymer chain can be regarded as a highly efficient transport medium of the electronic

excited states (excitons). As a result, binding events at a site might be sensed by a whole chain, leading to amplification of the fluorescent system.[6]

Interference experiments

To investigate the influence of other types of DNA on the fluorescence quenching of **P1** by ctDNA, we utilized three other DNA molecules: 5′-GGTGGCCATTACCTTTGACTCTTC-3′ with 24 bases (DNA-1), 5′-CCACCTGTTGGTAGTCCTTGTATTTAGTATCATC-3′ with 34 bases (DNA-2), and 5′-TGGTTCACGTAGTGGGCCATC-3 with 21 bases (DNA-3). Herein, interference experiments were performed in ethanol-Tris-HCl buffer to evaluate the sensing selectivity of **P1** toward ctDNA in the presence of equal concentrations of the three other DNA molecules. Sufficient fluorescence quench was observed for **P1** after the addition of ctDNA in the presence of various other DNA molecules (Figure 9), suggesting that the **P1** can be used as a selective fluorescent probe for ctDNA in the presence of other types of DNA that may compete with ctDNA to bind with **P1**.

CONCLUSIONS

In summary, the preparation of a novel conjugated poly(pyridinium salt)s derivative (**P1**) was described. The effects of solvent polarity and pH of the aqueous solution on the photophysical properties of **P1** were studied in detail. The ability of **P1** to bind ctDNA was explored by UV-Vis and fluorescence spectroscopy, CD and DLS. Because electrostatic interactions were expected to be the driving forces of the binding process, the investigations were performed in an ethanol-Tris-HCl buffer with pH 7.4, which is similar to the physiological pH. The adsorption quickly equilibrated, and a ctDNA-**P1** complex with nearly 1:1 stoichiometry was formed, as demonstrated by Job's plot based on the UV-Vis absorption data. The DLS data showed that aggregates formed upon the addition of ctDNA to **P1** in ethanol-Tris-HCl buffer, with a maximum mean diameter of 712 nm at the endpoint of the titration. Furthermore, the CD observation showed the structural alterations that the ctDNA underwent when it was bound to the conjugated polyelectrolyte **P1**; this finding indicates that the strong electrostatic attractions and intercalation interactions should be synergistically responsible for the binding of ctDNA to **P1**. The addition of ctDNA to **P1** in an ethanol-Tris-HCl buffer resulted in the fluorescence quenching of polymer **P1** with a large Stern–Volmer constant of $2.21 \times 10^5\ M^{-1}$. On the basis of the polymer fluorescence spectra response to the ctDNA concentration, we anticipate that this type of conjugated polyelectrolyte has ideal properties for use as DNA-sensitive optical probes for the detection or imaging of DNA.

CONFLICT OF INTEREST

The authors declare no conflict of interest.

ACKNOWLEDGEMENTS

We are grateful for the National Natural Science Foundation (51373122, 21074093) and the Program for New Century Excellent Talents in University (NCET-12-1066).

1 McQuade, D. T., Pullen, A. E. & Swager, T. M. Conjugated polymer-based chemical sensors. *Chem. Rev.* **100**, 2537–2574 (2000).
2 Thomas, S. W., Joly, G. D. & Swager, T. M. Chemical sensors based on amplifying fluorescent conjugated polymers. *Chem. Rev.* **107**, 1339–1386 (2007).
3 Achyuthan, K. E., Bergstedt, T. S., Chen, L., Jones, R. M., Kumaraswamy, S., Kushon, S. A., Ley, K. D., Lu, L., McBranch, D., Mukundan, H., Rininsland, F., Shi, X., Xia, W. & Whitten, D. G. Fluorescence superquenching of conjugated polyelectrolytes: applications for biosensing and drug discovery. *J. Mater. Chem.* **15**, 2648–2656 (2005).
4 Feng, X., Liu, L., Wang, S. & Zhu, D. Water-soluble fluorescent conjugated polymers and their interactions with biomacromolecules for sensitive biosensors. *Chem. Soc. Rev.* **39**, 2411–2419 (2010).
5 Zhu, C., Liu, L., Yang, Q., Lv, F. & Wang, S. Water-soluble conjugated polymers for imaging, diagnosis, and therapy. *Chem. Rev.* **112**, 4687–4735 (2012).
6 Zhou, Q. & Swager, T. M. Fluorescent chemosensors based on energy migration in conjugated polymers: the molecular wire approach to increased sensitivity. *J. Am. Chem. Soc.* **117**, 12593–12602 (1995).
7 Swager, T. M. The molecular wire approach to sensory signal amplification. *Acc. Chem. Res.* **31**, 201–207 (1998).
8 Lee, K., Povlich, L. K. & Kim, J. Recent advances in fluorescent and colorimetric conjugated polymer-based biosensors. *Analyst* **135**, 2179–2189 (2010).
9 Wang, L., Liu, X., Yang, Q., Fan, Q., Song, S., Fan, C. & Huang, W. A colorimetric strategy based on a water-soluble conjugated polymer for sensing pH-driven conformational conversion of DNA i-motif structure. *Biosens. Bioelectron.* **25**, 1838–1842 (2010).
10 Bao, B., Yuwen, L., Zheng, X., Weng, L., Zhu, X., Zhan, X. & Wang, L. A fluorescent conjugated polymer for trace detection of diamines and biogenic polyamines. *J. Mater. Chem.* **20**, 9628–9634 (2010).
11 Zhang, W., Zhu, L., Qin, J. & Yang, C. Novel Water-Soluble Red-Emitting Poly(p-phenylenevinylene) Derivative: Synthesis, Characterization, and Fluorescent Acetylcholinesterase Assays. *J. Phys. Chem. B* **115**, 12059–12064 (2011).
12 Zhang, W., Liu, L., Qin, J. & Yang, C. Water-soluble fluorene-based copolymers incorporated methoxyphenol moieties: Novel polymeric chemodosimeters for hypochlorous acid. *J. Polym. Sci., Part A: Polym. Chem* **50**, 1174–1180 (2012).
13 Zhang, W., Li, C., Qin, J. & Yang, C. Water-soluble poly(p-phenylene) incorporating methoxyphenol units: Highly sensitive and selective chemodosimeters for hypochlorite. *Polymer* **53**, 2356–2360 (2012).
14 Qin, C., Wu, X., Gao, B., Tong, H. & Wang, L. Amino acid-functionalized polyfluorene as a water-soluble Hg^{2+} chemosensor with high solubility and high photoluminescence quantum yield. *Macromolecules* **42**, 5427–5429 (2009).
15 Xu, B., Wu, X., Li, H., Tong, H. & Wang, L. Fluorescent detection of heparin by a cationic conjugated polyfluorene probe containing aggregation-induced emission units. *Polymer* **53**, 490–494 (2012).
16 Sun, P., Lu, X., Fan, Q., Zhang, Z., Song, W., Li, B., Huang, L., Peng, J. & Huang, W. Water-soluble iridium(III)-containing conjugated polyelectrolytes with weakened energy transfer properties for multicolor protein sensing applications. *Macromolecules* **44**, 8763–8770 (2011).
17 Gaylord, B. S., Heeger, A. J. & Bazan, G. C. DNA detection using water-soluble conjugated polymers and peptide nucleic acid probes. *Proc. Natl. Acad. Sci. USA* **99**, 10954–10957 (2002).
18 He, F., Tang, Y., Wang, S., Li, Y. & Zhu, D. Fluorescent amplifying recognition for DNA G-quadruplex folding with a cationic conjugated polymer: a platform for homogeneous potassium detection. *J. Am. Chem. Soc.* **127**, 12343–12346 (2005).
19 Hu, R., Liu, T., Zhang, X., Huan, S., Wu, C., Fu, T. & Tan, W. Multicolor fluorescent biosensor for multiplexed detection of DNA. *Anal. Chem.* **86**, 5009–5016 (2014).
20 Liu, B. & Bazan, G. C. Energy transfer between a cationic-conjugated poly(fluorene-co-phenylene) and thiazole orange for DNA hybridization detection involving G-rich sequences. *Macromol. Rapid Commun.* **28**, 1804–1808 (2007).
21 Liu, B. & Dishari, S. K. Synthesis, characterization, and application of cationic water-soluble oligofluorenes in DNA-hybridization detection. *Chem. Eur. J* **14**, 7366–7375 (2008).
22 Pu, K.-Y. & Liu, B. Intercalating dye harnessed cationic conjugated polymer for real-time naked-eye recognition of double-stranded DNA in serum. *Adv. Funct. Mater.* **19**, 1371–1378 (2009).
23 Chi, C., Mikhailovsky, A. & Bazan, G. C. Design of cationic conjugated polyelectrolytes for DNA concentration determination. *J. Am. Chem. Soc.* **129**, 11134–11145 (2007).
24 Peng, H., Soeller, C. & Travas-Sejdic, J. A novel cationic conjugated polymer for homogeneous fluorescence-based DNA detection. *Chem. Commun.* 3735–3737 (2006).
25 Ho, H. A., Dore, K., Boissinot, M., Bergeron, M. G., Tanguay, R. M., Boudreau, D. & Leclerc, M. Direct molecular detection of nucleic acids by fluorescence signal amplification. *J. Am. Chem. Soc.* **127**, 12673–12676 (2005).
26 Karlsson, K. F., Asberg, P., Nilsson, K. P. R. & Inganaes, O. Interactions between a zwitterionic polythiophene derivative and oligonucleotides as resolved by fluorescence resonance energy transfer. *Chem. Mater.* **17**, 4204–4211 (2005).
27 Ho, H.-A., Boissinot, M., Bergeron, M. G., Corbeil, G., Dore, K., Boudreau, D. & Leclerc, M. Colorimetric and fluorometric detection of nucleic acids using cationic polythiophene derivatives. *Angew. Chem., Int. Ed.* **41**, 1548–1551 (2002).
28 Baker, E. S., Hong, J. W., Gaylord, B. S., Bazan, G. C. & Bowers, M. T. PNA/dsDNA complexes: site specific binding and dsDNA biosensor applications. *J. Am. Chem. Soc.* **128**, 8484–8492 (2006).
29 Woo, H. Y., Vak, D., Korystov, D., Mikhailovsky, A., Bazan, G. C. & Kim, D.-Y. Cationic conjugated polyelectrolytes with molecular spacers for efficient fluorescence energy transfer to dye-labeled DNA. *Adv. Funct. Mater.* **17**, 290–295 (2007).
30 Liu, B. & Bazan, G. C. Tetrahydrofuran activates fluorescence resonant energy transfer from a cationic conjugated polyelectrolyte to fluorescein-labeled DNA in aqueous media. *Chem. Asian J.* **2**, 499–504 (2007).
31 Hong, J. W., Henme, W. L., Keller, G. E., Rinke, M. T. & Bazan, G. C. Conjugated-polymer/DNA interpolyelectrolyte complexes for accurate DNA concentration determination. *Adv. Mater.* **18**, 878–882 (2006).
32 Liu, B. & Bazan, G. C. Homogeneous fluorescence-based DNA detection with water-soluble conjugated polymers. *Chem. Mater.* **16**, 4467–4476 (2004).

33 Liu, B. & Bazan, G. C. Interpolyelectrolyte complexes of conjugated copolymers and DNA: platforms for multicolor biosensors. *J. Am. Chem. Soc.* **126**, 1942–1943 (2004).
34 Gaylord, B. S., Heeger, A. J. & Bazan, G. C. DNA hybridization detection with water-soluble conjugated polymers and chromophore-labeled single-stranded DNA. *J. Am. Chem. Soc.* **125**, 896–900 (2003).
35 Xu, Q.-H., Gaylord, B. S., Wang, S., Bazan, G. C., Moses, D. & Heeger, A. J. Time-resolved energy transfer in DNA sequence detection using water-soluble conjugated polymers: The role of electrostatic and hydrophobic interactions. *Proc. Natl. Acad. Sci. USA* **101**, 11634–11639 (2004).
36 Pu, K.-Y., Pan, S. Y.-H. & Liu, B. Optimization of interactions between a cationic conjugated polymer and chromophore-labeled DNA for optical amplification of fluorescent sensors. *J. Phys. Chem. B* **112**, 9295–9300 (2008).
37 Bazan, G. C. Novel organic materials through control of multichromophore interactions. *J. Org. Chem.* **72**, 8615–8635 (2007).
38 Lu, Y., Xiao, C., Yu, Z., Zeng, X., Ren, Y. & Li, C. Poly(pyridinium) salts containing calix [4]arene segments in the main chain as potential biosensors. *J. Mater. Chem.* **19**, 8796–8802 (2009).
39 Han, F., Lu, Y., Zhang, Q., Sun, J., Zeng, X. & Li, C. Homogeneous and sensitive DNA detection based on polyelectrolyte complexes of cationic conjugated poly(pyridinium salt)s and DNA. *J. Mater. Chem.* **22**, 4106–4112 (2012).
40 Sun, J., Lu, Y., Cheng, D., Sun, Y. & Zeng, X. Fluorescence turn-on detection of DNA based on the aggregation-induced emission of conjugated poly(pyridinium salt)s. *Polym. Chem* **4**, 4045–4051 (2013).
41 Wang, L., Li, Y., Sun, J., Lu, Y., Sun, Y., Cheng, D. & Li, C. Conjugated poly(pyridinium salt)s as fluorescence light-up probes for heparin sensing. *J. Appl. Polym. Sci.* **131**, 40933–40938 (2014).
42 Bhowmik, P. K., Han, Haesook, Cebe, J. J., Nedeltchev, I. K., Kang, S.-W. & Kumar, S. Synthesis and characterization of poly(pyridinium salt)s with organic counterions exhibiting both thermotropic liquid-crystalline and light-emitting properties. *Macromolecules* **37**, 2688–2694 (2004).
43 Nedeltchev, A. K., Han, H. & Bhowmik, P. K. Solution, thermal and optical properties of new poly(pyridinium salt)s derived from bisquinoline diamines. *Polym. Chem* **1**, 908–915 (2010).
44 Keshtov, M. L., Arslan Udumc, Y., Toppare, L., Kochurov, V. S. & Khokhlov, A. R. Synthesis of aromatic poly(pyridinium salt)s and their electrochromic properties. *Mater. Chem. Phys.* **139**, 936–943 (2013).
45 Nedeltchev, A., Han, H. & Bhowmik, P. K. Solution, thermal, and optical properties of poly(pyridinium salt)s derived from an ambipolar diamine consisting of diphenylquinoline and triphenyl amine moieties. *J. Polym. Sci. A: Polym. Chem* **48**, 4611–4620 (2010).
46 Zhao, C.-H., Wakamiya, A., Inukai, Y. & Yamaguchi, S. Highly emissive organic solids containing 2,5-diboryl-1,4-phenylene unit. *J. Am. Chem. Soc.* **128**, 15934–15935 (2006).
47 Chen, O., Cheng, Q. Y., Zhao, Y. C. & Han, B. H. Glucosamine hydrochloride functionalized water-soluble conjugated polyfluorene: synthesis, characterization, and interactions with DNA. *Macromol. Rapid Commun.* **30**, 1651–1655 (2009).
48 Zhang, W., Xu, L., Qin, J. & Yang, C. New water-soluble cationic poly(p-phenylenevinylene) derivative: the interaction with DNA and selective fluorescence enhancement induced by ssDNA. *Macromol. Rapid Commun.* **34**, 442–446 (2013).
49 Zhu, L., Yang, C. & Qin, J. An aggregation-induced blue shift of emission and the self-assembly of nanoparticles from a novel amphiphilic oligofluorene. *Chem. Commun.* 6303–6305 (2008).
50 Zhu, L., Zhong, C., Liu, Z., Qin, J. & Yang, C. New intramolecular through-space charge transfer emission: tunable dual fluorescence of terfluorenes. *Chem. Commun.* **46**, 6666–6668 (2010).
51 Tunis-Schneider, M. J. B. & Maestre, M. F. Circular dichroism spectra of oriented and unoriented deoxyribonucleic acid films-a preliminary study. *J. Mol. Biol.* **52**, 521–541 (1970).
52 Carvlin, M. J., Datta-Gupta, N. & Fiel, R. J. Circular dichroism spectroscopy of a cationic porphyrin bound to DNA. *Biochem. Biophys. Res. Commun.* **108**, 66–73 (1982).
53 Ivanov, V. I., Minchenkova, L. E., Schyolkina, A. K. & Poletayev, A. I. Different conformations of double-stranded nucleic acid in solution as revealed by circular dichroism. *Biopolymers* **12**, 89–110 (1973).
54 Matulis, D., Rouzina, I. & Bloomfield, V. A. Thermodynamics of cationic lipid binding to DNA and DNA condensation: Roles of electrostatics and hydrophobicity. *J. Am. Chem. Soc.* **124**, 7331–7342 (2002).
55 Lakowicz, J. R. *Principles of Fluorescence Spectroscopy* (Kluwer Academic, Plenum Publishers, New York, NY, USA, 1999).

Supplementary Information accompanies the paper on Polymer Journal website (http://www.nature.com/pj)